Synthesis, characterization and phosphotriesterase mimetic activity of some Zn(II) and Cu(II) complexes

ARTICLE *in* JOURNAL OF CHEMICAL SCIENCES · NOVEMBER 2013

Impact Factor: 1.19 · DOI: 10.1007/s12039-012-0331-4

5 AUTHORS, INCLUDING:

Mamata Singh
GITAM University
19 PUBLICATIONS **87** CITATIONS
SEE PROFILE

Ray J. Butcher
Howard University
1,042 PUBLICATIONS **9,379** CITATIONS
SEE PROFILE

Jerry P. Jasinski
Keene State College
647 PUBLICATIONS **2,571** CITATIONS
SEE PROFILE

Govindasamy Mugesh
Indian Institute of Science
155 PUBLICATIONS **4,320** CITATIONS
SEE PROFILE

J. Chem. Sci. Vol. 124, No. 6, November 2012, pp. 1301–1313.

Synthesis, characterization and phosphotriesterase mimetic activity of some Zn(II) and Cu(II) complexes

MAMATA SINGH[1], RAY J BUTCHER[2], JERRY P JASINSKI[3], JAMES A GOLEN[3] and GOVINDASAMY MUGESH[1,*]

[1]Department of Inorganic and Physical Chemistry, Indian Institute of Science, Bangalore 560 012, India
[2]Department of Chemistry, Howard University, Washington DC 20059, USA
[3]Department of Chemistry, Keene State College, Keene, NH 03453–2001, USA
e-mail: mugesh@ipc.iisc.ernet.in

Abstract. We report here the synthesis and characterization of a few phenolate-based ligands bearing tert-amino substituent and their Zn(II) and Cu(II) metal complexes. Three mono/binuclear Zn(II) and Cu(II) complexes $[Zn(L1)(H_2O)].CH_3OH.H_2O$ **(1)** (**H_2L1** = 6,6′-(((2-dimethylamino)ethylazanediyl)*bis*(methylene))*bis*(2,4-dimethylphenol), $[Zn_2(L2)_2]$ **(2)** (**H_2L2** = 2,2′-(((2-dimethylamino)ethyl)azanediyl)*bis*(methylene)*bis*(4-methylphenol) and $[Cu_2(L3)_2.CH_2\ Cl_2]$ **(3)** (**H_2L3** = (6,6′-(((2-(diethylamino)ethyl)azanediyl)*bis*(methylene))*bis*(methylene))*bis*(2,4-dimethylphenol) were synthesized by using three symmetrical tetradendate ligands containing N_2O_2 donor sites. These complexes are characterized by a variety of techniques including; elemental analysis, mass spectrometry, ^{1}H, ^{13}C NMR spectroscopic and single crystal X-ray analysis. The new complexes have been tested for the phosphotriesterase (PTE) activity with the help of ^{31}P NMR spectroscopy. The ^{31}P NMR studies show that mononuclear complex $[Zn(L1)(H_2O)].CH_3OH.H_2O$ **(1)** can hydrolyse the phosphotriester i.e., p-nitrophenyl diphenylphosphate (PNPDPP), more efficiently than the binuclear complexes $[Zn_2(L2)_2]$ **(2)** and $[Cu_2(L3)_2.CH_2Cl_2]$ **(3)**. The mononuclear Zn(II) complex **(1)** having one coordinated water molecule exhibits significant PTE activity which may be due to the generation of a Zn(II)-bound hydroxide ion during the hydrolysis reactions in CHES buffer at pH 9.0.

Keywords. *Bis*-phenolate ligand; Zn(II) complex; mononuclear complex; binuclear complex; crystal structure; PTE activity.

1. Introduction

Zinc is one of the essential trace elements and second most abundant transition metal in several important biological processes.[1] This element is important for the growth, development and differentiation of all types of life including microorganisms, plants and animals.[2] The strong Lewis acidity, rapid ligand exchange, flexible coordination geometry, lack of redox property and 'borderline' hard-soft behaviour make zinc as a suitable element for biological systems.[3] Zinc hydrolases are enzymes that contain zinc(II) at the active site and that catalyse a variety of hydrolytic reactions involving many different substrates.[4] Examples of some well-studied zinc(II) enzymes include carboxypeptidase,[5] D,D carboxypeptidase,[6] metallo-β-lactamase[7] and phosphotriesterase (PTE).[8] PTE, isolated from soil bacteria, is a binuclear zinc(II) enzyme[9], which catalyses the hydrolysis of a wide range of organophosphate esters, including agricultural pesticides and chemical warfare agents (scheme 1).[10–12] To date, the natural substrate for PTE is not known. The active site of PTE consists of a binuclear zinc(II) metal ion bound to water or hydroxyl bridging group with Zn…Zn distances ranging from 3.0 to 3.5 Å[13] (figure 1). The inactivation of phosphotriesters is important as the accumulation of these organophosphate pesticides result in irreversible inactivation of the acetylcholinesterase (AChE),[14] which is a key enzyme for nerve function in living systems. PTE is known to hydrolyse these toxic organophosphorus compounds (triester) to less toxic diesters (scheme 1).[15,16] The inhibition/inactivation of AChE by organophosphates leads to increase in the concentration of acetylcholine, which results in nerve failure, paralysis and ultimately such inhibition leads to death.

The design and synthesis of metal complexes that can hydrolyse phosphotriesters have attracted considerable attention.[17] Among them, only few complexes have been shown to catalyse the hydrolysis of phosphotriesters at ambient conditions.[18] Recently, we have reported some zinc(II) complexes as models for PTE

*For correspondence

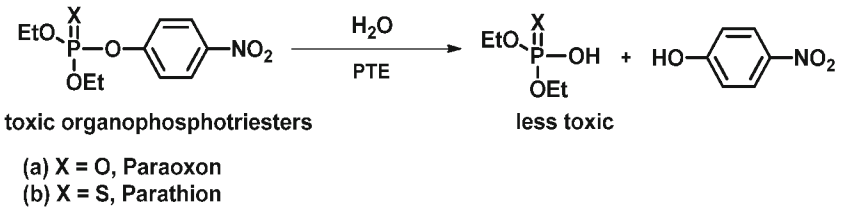

Scheme 1. Hydrolysis of Paraoxon or parathion by phosphotriesterase to harmless product.

at ambient conditions.[19] The use of chelating tetradenate amine-*bis*(phenolate) ligands for the synthesis of metal complexes is an important area of research in transition metal chemistry.[20] Particularly, such ligands have been used frequently for the synthesis of metal-based catalysts containing first-row transition metals.[21,22] Recently, copper(II)-bisphenolate complexes have been used as functional models for various biomolecules.[23] In continuation of our work on the development of functional models for zinc hydrolases, particularly PTE, we have synthesized a few *bis*-phenolate ligands and their Zn(II) and Cu(II) complexes and studied the PTE activity of these complexes.

2. Experimental

2.1 *General methods and materials*

2,4-Dimethyl phenol, N,N-dimethylethylenediamine, N,N-diethylethylenediamine, CHES buffer, and diphenyl phosphoryl chloride were purchased from Sigma-Aldrich chemical company. 4-Methylphenol and NaOH were purchased from Sisco Research Laboratories. $ZnCl_2$ (anhydrous), $CuCl_2.2H_2O$ and triethylamine were purchased from Merck, Sd-fine and Fluka, respectively and used as such for reactions. Solvents were purified by standard procedures and were freshly distilled prior to use. Ultrapure Milli-Q water (18.2 mΩ) was used in all PTE experiments. All reactions were carried out at room temperature unless it is mentioned. ^{1}H NMR (400 MHz), ^{13}C (100.56 MHz) and ^{31}P (161.9 MHz) NMR spectra were obtained on Bruker 400 MHz NMR spectrometer. Chemical shifts are cited in ppm with respect to $SiMe_4$ as internal (^{1}H and ^{13}C) and phosphoric acid (^{31}P) as external standard. The deuterated solvents DMSO-d_6, $CDCl_3$ and D_2O were purchased from Sigma-Aldrich chemical company. Mass spectral studies were carried out on a Q-TOF micro mass spectrometer or on a Bruker Daltonics 6000 plus mass spectrometer with ESI-MS mode analysis. The ligands **H_2L1** and **H_2L3** were synthesized by using literature method used for the related ligands with minor modifications[24] and p-nitrophenyl diphenylphosphate (PNPDPP) was prepared by reported procedure.[25]

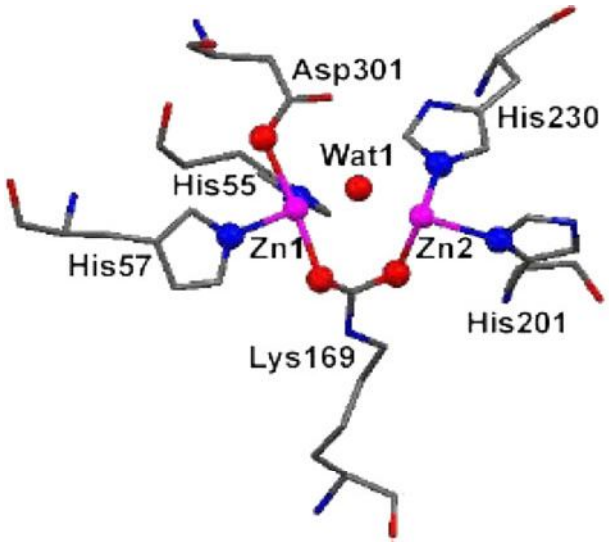

Figure 1. The binuclear active site of phosphotriesterase from *Pseudomonas diminuta*. PDB code for structure is 1HZY.[13]

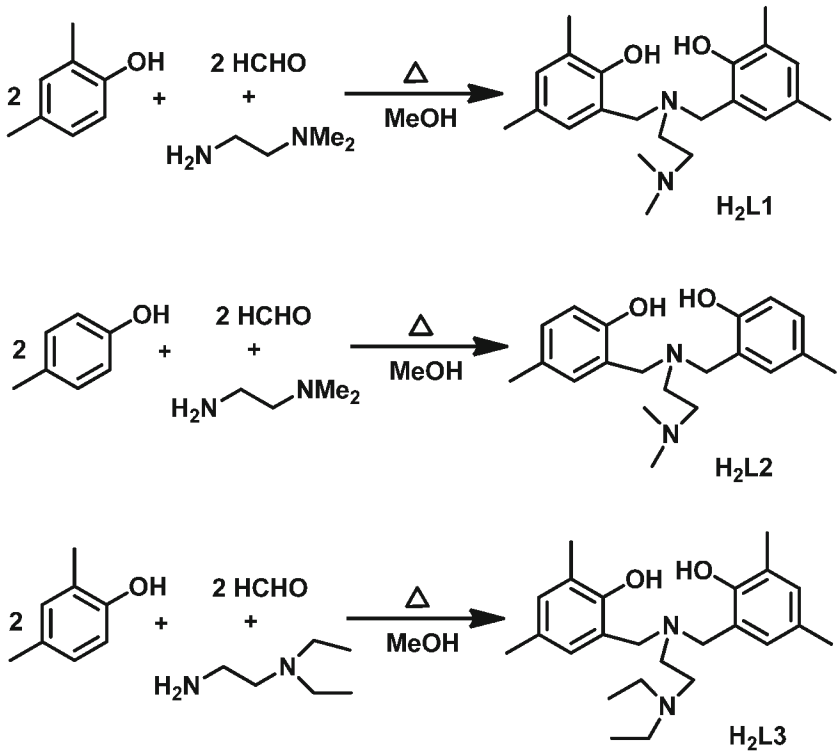

Scheme 2. Schematic representation for synthesis of ligands **H_2L1–H_2L3**.

2.2 *Synthesis of ligand* ***H_2L1***

A solution of 2,4-dimethylphenol (2.5 g, 30 mmol), *N*, *N*−dimethylethylenediamine (1.1 mL, 15 mmol) and 37% aqueous formaldehyde (2.4 mL, 42 mmol) in methanol (30 mL) was refluxed with stirring for 24 h. The mixture was cooled and the product was filtered and washed with ice-cold methanol to give the colourless *bis*-phenolate ligand. mp: 175–176°C (lit [24]: 174°C), Yield: 3.0 g, 84%. Anal. calcd. for $C_{22}H_{32}N_2O_2$ (356.50): C, 74.12; H, 9.05; N, 7.86; found: C, 74.03; H, 8.73; N, 7.97. ^{1}H NMR ($CDCl_3$, ppm): δ 2.19 (s, 12H), 2.30 (s, 6H), 2.54 (s, 4H), 3.56 (s, 4H), 6.66 (s, 4H), 6.84 (s, 4H); ^{13}C NMR ($CDCl_3$, ppm): δ 16.7, 20.9, 45.5, 49.5, 56.8, 122.0, 125.9, 127.8, 128.8, 131.6, 153.1. ESI-MS (m/z) for calcd. $C_{22}H_{32}N_2O_2$: 356.50, found: 356.99 [M^+]. The structures of ligand **H_2L1** are given in scheme 2 and figure 2a.

2.3 *Synthesis of ligand* ***H_2L2***

A solution of p-cresol (3 mL, 28.7 mmol), *N*,*N*-dimethylethylenediamine (1.5 mL, 14.3 mmol) and 37% formaldehyde (1.1 mL, 40 mmol) in methanol (20 mL) was refluxed with stirring for 24 h. The mixture was allowed to attain room temperature. The filtrate was kept as such at room temperature for crystallization. After 20 days, the *bis*-phenolate ligand was obtained as white crystals. mp: 118–120°C, Yield: 1.77 g, 57%. Anal. calcd. for $C_{20}H_{28}N_2O_2$ (328.44): C, 73.14; H, 8.59; N, 8.53; found: C, 72.77; H, 8.14; N, 8.60. ^{1}H NMR ($CDCl_3$, ppm): δ 2.22 (s, 6H), 2.30 (s, 6H) 2.58–2.60 (m, 4H), 3.59 (s, 4H), 6.76 (s, 4H), 6.82 (s, 4H), 6.97 (s, 4H); ^{13}C NMR ($CDCl_3$, ppm): δ 20.9, 45.4, 49.6, 56.6, 117.1, 122.6, 128.5, 130.4, 131.2, 155.0. ESI-MS (m/z) for calcd. $C_{20}H_{28}N_2O_2$: 328.45, found: 328.96 [M^+]. The structures of ligand **H_2L2** are given in scheme 2 and figure 2b.

2.4 *Synthesis of ligand* ***H_2L3***

A solution of 2,4-dimethylphenol (2.5 g, 41 mmol), *N*,*N*−diethylethylenediamine (1.5 mL, 20.6 mmol) and 37% aqueous formaldehyde (2.5 mL, 60 mmol) in methanol (30 mL) was refluxed with stirring for 24 h. The reaction mixture was cooled and filtered off. The residue obtained was washed with ice-cold methanol to give the *bis*-phenolate ligand as white solid. The crystals suitable for X-ray analysis were obtained from a $CHCl_3$ solution. mp: 142–144°C (lit[24]: 143°C) Yield: 2.0 g, 80%. Anal. calcd for $C_{24}H_{36}N_2O_2$ (385.50): C, 74.96; H, 9.44; N, 7.28; found: C, 74.72; H, 9.00; N, 7.51. ^{1}H NMR ($CDCl_3$, ppm): δ 1.08–1.13 (t, 6H), 2.19 (s, 12H), 2.53–2.58 (m, 4H), 2.62–2.63 (t, 4H), 3.56

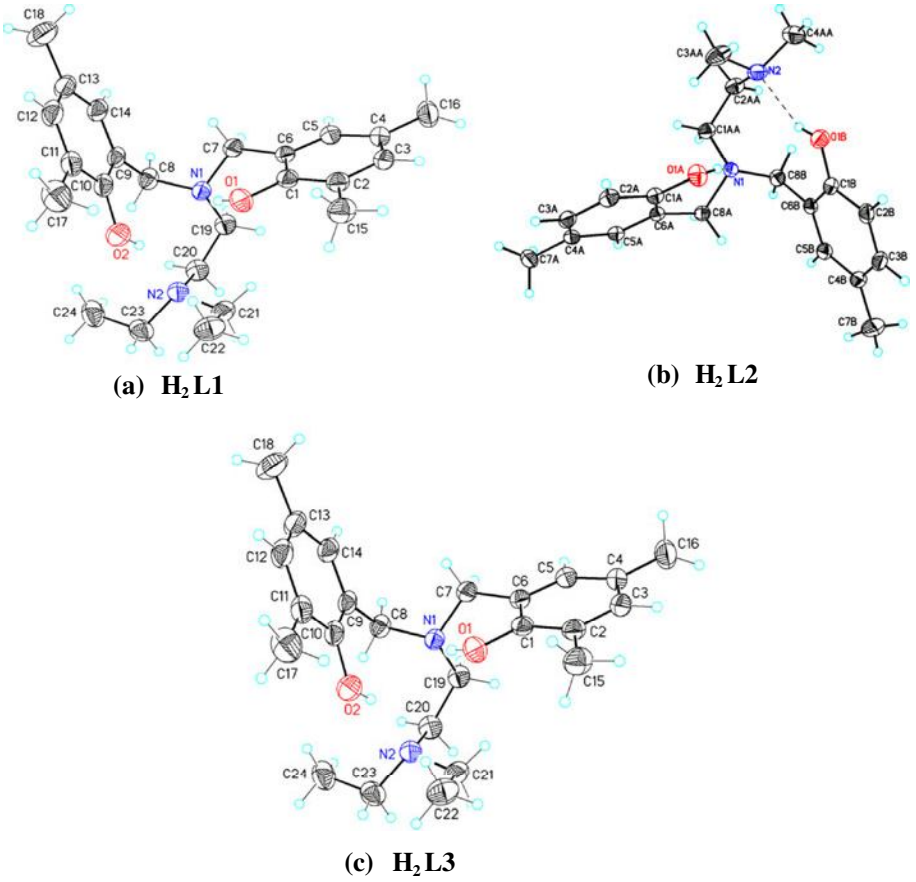

(a) H_2L1 **(b) H_2L2**

(c) H_2L3

Figure 2. X-ray crystal structures of ligands **H_2L1**, **H_2L2** and **H_2L3** with atom labelling scheme at 50% probability.

(s, 4H), 6.67 (s, 2H), 6.84 (s, 2H), 9.36 (br s, 2H); ^{13}C NMR ($CDCl_3$, ppm): δ 10.4, 16.6, 20.9, 46.1, 49.2, 50.3, 56.2, 121.9, 125.9, 127.7, 128.7, 131.5, 153.1. ESI-MS (m/z) for calcd. $C_{24}H_{36}N_2O_2$: 384.55, found: 385.07 [M^+]. The structures of ligand **H_2L3** are given in scheme 2 and figure 2c.

2.5 *Synthesis of complex [Zn(L1).H_2O].CH_3OH.H_2O (1)*

A methanolic solution of the ligand **H_2L1** (0.356 g, 0.5 mmol) was treated with NaOH (0.80 g, 1 mmol) in distilled water (5 mL) for 2 h to obtain the corresponding sodium phenolate. To this, anhydrous $ZnCl_2$ (0.136 g, 0.5 mmol) was added in methanol (10 mL). The resulting colourless solution was stirred and refluxed at 60–70°C. The solvent was evaporated under reduced pressure to give a colourless solid which was crystallized from methanol:diethylether (50:50 v/v) to give colourless needle shaped X-ray quality crystals. mp: >255°C, Yield 0.46 g, 52%. Anal. calcd. for $C_{22}H_{30}N_2O_2Zn.CH_3OH.2H_2O$ (487.92): C, 56.61; H, 7.85; N, 5.74; found: C, 55.52; H, 7.56; N, 5.72. ^{1}H NMR ($CDCl_3$, ppm): δ 2.19 (s, 12H), 2.02 (s, 6H), 2.56–2.59 (m, 4H), 4.20, 4.17 (s, 2H), 3.85 (s, 4H), 6.64 (s, 2H), 6.86 (s, 2H); ^{13}C NMR ($CDCl_3$, ppm): δ 17.8, 20.8, 46.0, 58.8, 62.0, 123.3, 124.2, 128.1, 129.4, 132.0, 161.7. ESI-MS (m/z) for calcd. [Zn(L1)] + Na^+: 441.16, found: 441.04 [M^+]; ESI-MS (m/z) for calcd. [Zn(L1) + $2H_2O$]: 455.93, found: 455.0 [M^-]. The structure of complex **1** is given in figure 3.

2.6 *Synthesis of complex [$Zn_2(L2)_2$] (2)*

A methanolic solution of the ligand **H_2L2** (0.328 g, 1 mmol) was treated with NaOH (0.80 g, 2 mmol) in water (5 mL) for 2 h to obtain corresponding sodium phenolate. To this anhydrous $ZnCl_2$ (0.136 g, 1 mmol) was added in methanol (10 mL), resulting in a yellowish solution. The mixture was stirred and refluxed at 60–70°C for 3 h. The resulting turbid solution containing the complex [$Zn_2(L2)_2$] **(2)** was filtered. The solvent was evaporated under reduced pressure to give [$Zn_2(L2)_2$] **(2)** as a white solid.

The solid product was dissolved in CH_3OH:H_2O (95:5, v/v) and kept for crystallization. Upon standing at room temperature, the product crystallized out as

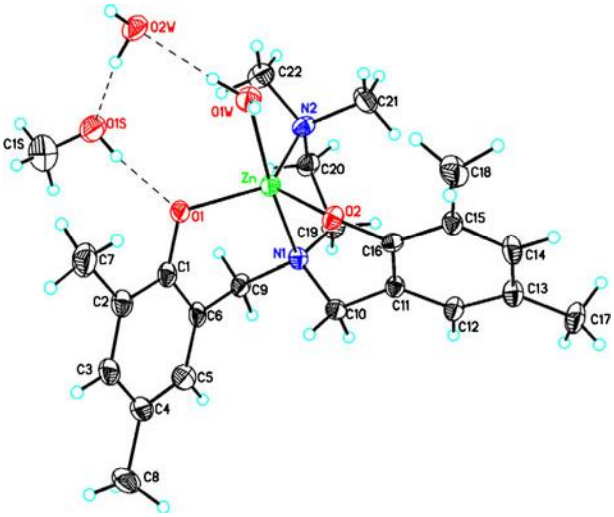

Figure 3. X-ray crystal structure of complex $[Zn(L1).H_2O].CH_3OH.H_2O$ **(1)** with atom labelling scheme at 50% probability.

white square plate crystals suitable for X-ray analysis. mp: 264–266°C, Yield: 0.28 g, 86%. Anal. calcd. for $C_{40}H_{52}N_4O_4Zn_2$ (783.60): C, 61.30; H, 6.69; N, 7.15; found: C, 60.62; H, 7.07; N, 7.02. ^{1}H NMR (CD_3OD, ppm): δ 6.85, 6.54 (d,d 2H, 2H), 3.24 (s, 4H), 2.08 (m, 4H), 2.25 (s, 12H), 2.23 (s, 3H). ESI-MS (m/z) for calcd. [Zn(L2)]: 390.13, found: 390.92 [M^+]; ESI-MS (m/z) for calcd. [Zn(L2)] + Na^+: 413.12, found: 412.92. The structure of complex **2** is given in figure 4a.

2.7 *Synthesis of complex $[Cu_2(L3)_2]CH_2Cl_2$ (3)*

The ligand **H_2L3** (0.384 g, 1 mmol) (in methanol: dichloromethane) (25 mL, 50:50 v/v) and triethylamine (280 μl, 2 mmol) (in methanol) were mixed and the reaction mixture was stirred for 2 h to obtain the deprotonated ligand L3. $CuCl_2.2H_2O$ (0.170 g, 1 mmol) in methanol (10 mL) was added to the reaction mixture. The resulting dark brown solution was stirred and refluxed for 2 h and then the solvent was removed under pressure to afford a brown solid. The resulted brown solid was dissolved in dichloromethane: methanol (50:50 v/v) to get good quality crystals by diffusion method. mp: 208–210°C, Yield: 0.364 g, 95%. Anal. calcd. for $C_{48}H_{68}N_4O_4Cu_2$(977.07): C, 64.62; H, 7.68; N, 6.28; found: C, 63.99; H, 7.17; N, 6.12. ESI-MS (m/z) for calcd. [Cu(L3)]: 445.19, found: 446.33 [M^+]; ESI-MS (m/z) for calcd. [Cu(L3)] + Na^+: 468.18, found: 468.13. The structure of complex **3** is given in figure 5a.

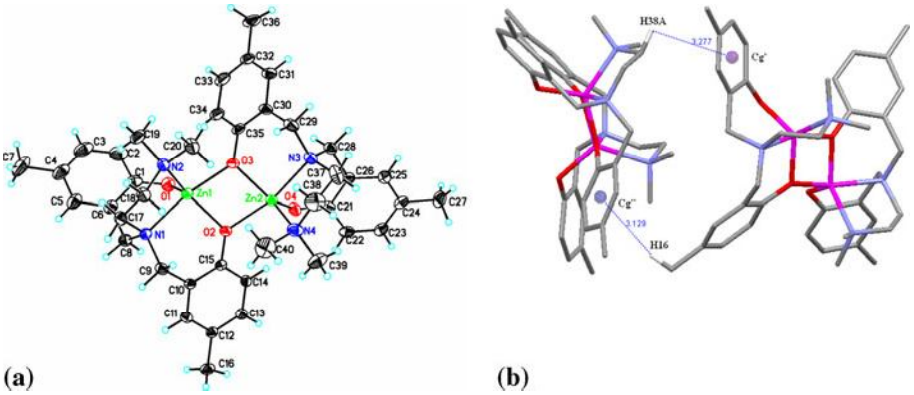

Figure 4. (**a**) X-ray crystal structure of complex $[Zn_2(L2)_2]$ **(2)** with atom labelling scheme at 50% probability. (**b**) The presence of C–H…π interactions in complex $[Zn_2(L2)_2]$ **(2)**. Hydrogen atoms except H16 and H38A are omitted for clarity.

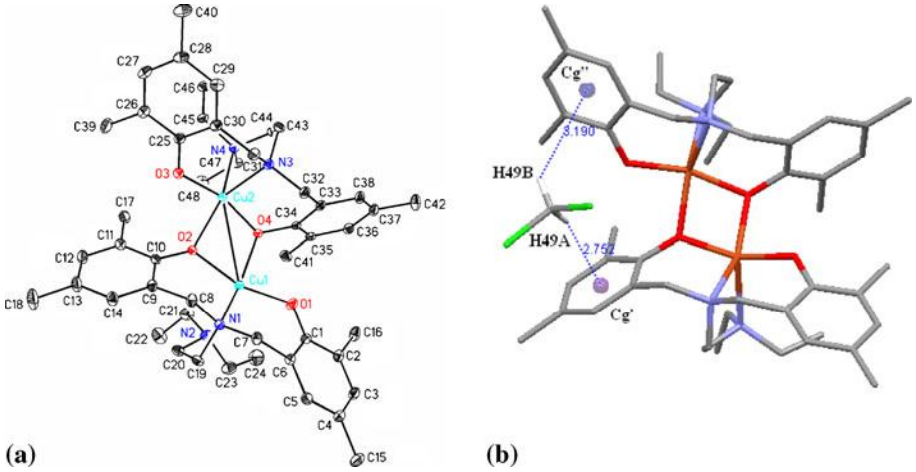

Figure 5. (**a**) X-ray crystal structure of complex $[Cu_2(L2)_2]$ **(3)** with atom labelling scheme at 50% probability. The solvent molecule is omitted for clarity. (**b**) The presence of C–H...π interactions in complex $[Cu_2(L3)_2].CH_2Cl_2$ **(3)**. Hydrogen atoms except H49A and H49B are omitted for clarity.

2.8 *Single crystal X-ray crystallography*

X-ray crystallographic studies for ligand **H_2L2**, complexes **1** and **2** were carried out on a Bruker Apex-II diffractometer at ambient temperature 296(2) K and for the ligand **H_2L3** and the complex **3**, the data collection was performed at temperature 298(2) and 173(2), respectively with a graphite monochromated MoKα (λ = 0.71073 Å) radiation source. The data refinement and reduction were performed by using standard procedure[26] for **H_1L3** and complex **3**. The structures were solved by direct methods (*SHELX* 97) and refined against all data by full matrix least square on F^2 using anisotropic displacement parameter for all non-hydrogen atoms. All hydrogen atoms were included in the refinement at geometrically ideal positions and refined with a riding model.[27,28] Empirical absorption corrections were applied to all structures using *SADABS*.[29] The perspective views of all reported compounds were obtained by using *ORTEP* program.[30] The crystallographic data and structural refinement details for ligands **H_2L2-H_2L3** and complexes **1–3**, are given in tables 1 and 2, respectively.

2.9 *Phosphotriestrase activity*

The PTE activity of complexes **1–3** was studied by employing ^{31}P NMR spectroscopy method. The hydrolysis of *p*-nitrophenyl diphenylphosphate (PNPDPP) by the zinc(II) and copper(II) complexes was determined by ^{31}P method.[19] The PTE activity of complexes was monitored by the disappearance of PNPDPP (triester) peak around −18.01 ppm and the appearance of a new peak for PNP (diester) around −10.01 ppm. In each case, the possible conversion of diester to the corresponding monoester was not monitored by ^{31}P NMR spectroscopy.

Table 1. Crystallographic data for ligands **H_2L2–H_2L3**.

	H_2L2	**H_2L3**
Empirical formula	$C_{20}H_{28}N_2O_2$	$C_{24}H_{36}N_2O_2$
Fw	328.44	384.55
T(K)	296(2)	298(2)
γ (″)	0.71073	0.71073
Crystal system	Monoclinic	Orthorhombic
Space group	P 21/c	Pbca
a (″)	14.920(8)	14.0580(8)
b (″)	6.202(3)	16.1583(11)
c (″)	22.102(13)	20.4824(11)
β (deg)	108.959(10)	–
V (″^{3})	1934.1(19)	4652.6(5)
Z	4	8
D_{calcd}/g cm^{-3}	1.128	1.098
F(000)	712	1680
μ (mm^{-1})	0.073	0.069
θ range (deg)	1.44 to 25.35	3.07 to 27.88
Reflections measured	13623	51689
Reflections used	3546	5548
Parameters	238	265
R1	0.0758	0.0588
wR2	0.1362	0.1517
Goodness of fit on F^2	1.042	1.028

Table 2. Crystallographic data for complexes **1**, **2** and **3**.

	$[Zn(L1).H_2O].CH_3OH.H_2O$ **1**	$[Zn_2(L2)_2]$ **2**	$[Cu_2(L2)_2]CH_2Cl_2$ **3**
Empirical formula	$C_{23}H_{38}N_2O_5Zn$	$C_{40}H_{52}N_4O_4Zn_2$	$C_{49}H_{70}ClCu_2N_4O_4$
Fw	487.92	783.60	977.07
T(K)	296(2)	293(2)	173(2)
γ (″)	0.71073	0.71073	0.71073
Crystal system	Orthorhombic	Monoclinic	Triclinic
Space group	P212121	P 21/c	P-1
a (Å)	7.5481(15)	10.5300(5)	12.5419(7)
b (Å)	14.063(3)	16.2267(8)	13.0122(9)
c (Å)	23.994(5)	24.2885(12)	15.6606(10)
α (deg)	–	–	93.548(5)
β (deg)	–	94.790(3)	102.922(5)
γ (deg)	–	–	103.509(5)
V (Å^3)	2546.9(9)	4135.6(3)	2404.5(3)
Z	4	4	2
D_{calcd}/g cm^{-3}	1.272	1.259	1.350
F(000)	1040	1648	1032
μ (mm^{-1})	0.997	1.201	1.042
θ range (deg)	1.70 to 25.25	1.51 to 25.25	3.24 to 28.70
Reflections measured	8772	29500	21148
Reflections used	4573	7269	12010
Parameters	300	459	562
R1	0.0677	0.0527	0.0372
wR2	0.1186	0.1188	0.0899
Goodness of fit on F^2	0.918	0.966	1.018

3. Results and discussion

3.1 *Synthesis*

The tetradentate *bis*-phenolate family of ligands is synthesized from readily available starting materials; primary amines, formaldehyde and substituted phenols, in a single step using the Mannich-type condensation method. The symmetric ligands **H_2L1** and **H_2L3** were prepared by following a method reported in the literature with minor modifications.[24] These ligands were prepared in methanol under reflux conditions. The schematic representation for the synthesis of ligands **H_2L1-H_2L3** is shown in scheme 2. The ligand **H_2L2** was synthesized by addition of *N*,*N*-dimethylethylenediamine and formaldehyde to a methanolic solution of 4-methylphenol (*p*-cresol). On the other hand, ligands **H_2L1** and **H_2L3** were prepared by addition of *N*,*N*-dimethylethylenediamine or *N*,*N*-diethylethylenediamine, respectively, to a methanolic solution of formaldehyde and 2,4-dimethylphenol. The *bis*-phenolate ligands **H_2L1-H_2L3** were chosen for this study as the tetradentate N_2O_2 systems can hold two metal ions together for the hydrolysis reactions. It is well-established that suitably designed phenolate ligands with ethylenediamine arms strongly favour the formation of binuclear complexes.[31] Therefore, we thought it is worthwhile to utilize the ligands **H_2L2** and **H_2L3** to synthesize some binuclear zinc(II) and copper(II) complexes. The complexes **1–3** were synthesized by treating the appropriate ligands (**H_2L1-H_2L3**) with bases such as NaOH or triethylamine under reflux conditions, followed by treatment with suitable metal halides. The crystals of these complexes were obtained by slow evaporation method or vapour diffusion. The crystals of complexes **1** and **2** obtained by a slow evaporation method using MeOH and MeOH:H_2O (90:10, v:v), respectively. For complex **3**, suitable crystals were obtained by diffusion method using MeOH:DCM (50:50 v:v).

3.2 *Single X-ray crystal structures*

3.2a *Crystal structure of ligands* **H_2L^1- H_2L^3**: The crystal structure of **H_2L^1-H_2L^3** is shown together with atom labelling scheme in figure 2. The bond lengths and angles are in the normal range observed for other related compounds. The intramolecular N–H…O hydrogen bonds are shown in table 3. The distances observed for

Table 3. Hydrogen bonds for ligands $\mathbf{H_2L^1}$-$\mathbf{H_2L^3}$ [Å].

Bond lengths (D-H...A) [Å]		
$\mathbf{H_2L^1}$	O(1)-H(10)...N(2)	1.95(1)
	O(2)-H(20)...N(1)	1.97(1)
$\mathbf{H_2L^2}$	O(1A)-H(1A)...N(1)	1.97(1)
	O(1B)-H(1B)...N(2)	2.03(1)
$\mathbf{H_2L^3}$	O(1)-H(10)...N(1)	1.98(1)
	O(2)-H(20)...N(2)	1.98(1)

these hydrogen bonds are comparable in $\mathbf{H_2L^1}$-$\mathbf{H_2L^3}$ (table 3).

3.2b *Crystal structure of complex [Zn(L1).H_2O].H_2O.CH_3OH (1)*: The structural analysis reveals that [Zn(L1).H_2O].H_2O.CH_3OH **(1)** crystallizes in an orthorhombic crystal system with space group $P2_12_12_1$. An ellipsoid plot for the crystal structure of molecule with the numbering scheme is depicted in figure 3. The details of crystal data are listed in table 2 and the selected bond lengths and bond angles are listed in table 4. The single crystal X-ray data confirm the formulation of complex **1** as mononuclear zinc(II) with one deprotonated ligand L1 and one coordinated H_2O molecule. Furthermore, the complex **1** has distorted trigonal bipyramidal geometry around the metal centre. The two phenolate oxygen atoms and a nitrogen atom (N2) form the trigonal plane, whereas the oxygen atom of coordinated H_2O molecule and the nitrogen atom of ethylene side arm occupy the axial coordination sites. The Zn(II) is nearly coplanar with the three atoms forming trigonal plane (O1O2N2). The angle between the two mean planes bearing the two symmetry related phenyl rings is ~66.21°. The two phenyl rings in the complex are planar and completely retain their aromaticity. The observed Zn–O bond distances [Zn-O1 = 1.953(15) Å, Zn-O2 = 1.962(6) Å] in complex **1** are comparable to the Zn–O bond distances reported in literature.[32]

Similarly, the Zn-N1 = 2.205(5) and Zn-N2 = 2.094(8) distances are almost comparable to the reported Zn–N bond distances in related coordination complex.[32] The N1–Zn–O(1W) axial bond angles demonstrate the distortion of molecule from ideal geometry, with the two small oxygen atoms bent away from Zn–N_{axial} bond. The Zn–O–C bond angles [Zn-O2-C16 = 122.23° and Zn-O1-C1 = 117.43°] are quite closer to the ideal value of 120° for sp^2 hybridized phenolate oxygen atom. A comparison of Zn-O(1W) = 2.144(5) bond length with similar systems shows that the value is in good agreement with those reported in the literature.[33,34] The complex **1** has one metal-bound water molecule similar to that in the active site of PTE enzymes. The hydrogen bonds present in complex **1** are listed in table 5.

3.2c *Crystal structure of complex [$Zn_2(L2)_2$] (2)*: The crystal structure refinement data related to complex **2** are given in table 2 and the main bond distances, bond angles are listed in table 6. The C–H...π interactions are listed in table 6. The coordination sites of ligand $\mathbf{H_2L2}$ are represented in figure 4a. The title complex [$Zn_2(L2)_2$] **(2)** crystallizes in monoclinic system with space group $P2_1/c$ with Z = 4. The symmetric unit of complex consists of a dinuclear $\mathbf{[Zn_2(L2)_2]}$ molecule with two phenolate oxygen atoms acting as a $(\mu\text{–O})_2$ bridge between the metal centre. The coordination geometry about the Zn centres can be described as distorted square pyramidal with two amine nitrogen and two bridging oxygen atoms [O(2)O(3)N(3)N(4) around Zn(1) metal ion centre and N(3)O(3)O(2)N(4) around Zn(2) metal ion centre]. The Zn–O(phenolic) bond lengths in complex **2**, which lie in the range 1.936(3)–2.047(3) Å, are almost identical to the Zn–O(phenolic) bond lengths reported

Table 4. Selected bond lengths [Å] and angles (°) for complex [Zn(L1).H_2O].H_2O.CH_3OH **(1)**.

Bond lengths [Å]			
Zn-O(1)	1.95(5)	Zn-N(2)	2.09(8)
Zn-O(2)	1.96(6)	Zn-N(1)	2.20(5)
Zn-O(1W)	2.14(5)		
Angles (°)			
O(1)-Zn-O(2)	123.20(3)	O(1)-Zn-N(1)	92.30(2)
O(1)-Zn-N(2)	118.20(3)	O(2)-Zn-N(1)	92.10(2)
O(2)-Zn-N(2)	118.60(2)	N(2)-Zn-N(1)	83.30(3)
O(1)-Zn-O(1W)	92.80(2)	O(1W)-Zn-N(1)	172.40(3)
O(2)-Zn-O(1W)	89.90(2)	C(1)-O(1)-Zn	117.40(5)
N(2)-Zn-O(1W)	89.20(3)	C(16)-O(2)-Zn	122.20(5)

Table 5. Hydrogen bonds for complex **1** [Å and °].

D-H...A	d(D-H)	d(H...A)	d(D...A)	<(DHA)
O(1S)-H(1S)...O(1)	0.82(1)	1.80(1)	2.61(1)	168.40(1)
O(1W)-H(1W1)...O(2W)#1	0.82(2)	1.93(3)	2.71(1)	161.00(1)
O(1W)-H(1W2)...O(2W)	0.82(2)	1.93(2)	2.73(1)	170.00(1)
O(2W)-H(2W1)...O(2)#2	0.82(2)	2.09(8)	2.70(7)	131.00(1)
O(2W)-H(2W2)...O(1S)	0.83(2)	1.88(4)	2.65(8)	157.00(9)

Symmetry transformations used to generate equivalent atoms:
#1 x+1/2,−y+3/2,−z+2 #2 x−1/2,−y+3/2,−z+2

in literature.[35] The Zn–N bond lengths range between 2.157(4) and 2.192(3) Å. However, the Zn...Zn distance [3.155(7)] in complex **2** is shorter than that of binuclear PTE (3.46 Å).[13] The crystal packing of complex **2** reveals the existence of C–H...π intermolecular interactions. There are two types of C–H...π interactions present in the molecule, C16-H16...C33 (2.813 Å) and C38-H38A...C4 (2.889 Å). The centroid distances with C–H are C38-H38...$Cg'_{(4mp)}$ = 3.276 Å ($Cg'_{(4mp)}$= C1C2C3C4C5C6)) and C16-H16...$Cg''_{(4mp)}$= 3.130 Å ($Cg''_{(4mp)}$ = C33C31C30C35C34 C33) (figure 4b). In complex **2**, the dihedral angle between two square basal planes [N(1)O(2)O(3)N(2) at Zn(1) and N(3)N(4)O(2)O(3) at Zn(2)] is ∼ 59.30°.

3.2d *Crystal structure of complex $[Cu_2(L3)_2].CH_2Cl_2$ (3)*: The crystal structure refinement data related to complex **3** is given in table 2 and significant bond distances and bond angles are listed in table 7. The C–H...π interactions are listed in table 8. The coordination sites of ligand **H_2L3** are represented in figure 5a. The title complex $[Cu_2(L3)_2].CH_2Cl_2$ **(3)** crystallizes in the triclinic system with space group P-1 with Z = 2. The symmetric unit of complex consists of a dinuclear $[Cu_2(L3)_2]$ molecule with two phenolate oxygen atoms acting as a $(\mu\text{–O})_2$ bridge between the Cu(II) metal centre. The coordination geometry about the Cu centres can be described as distorted square pyramidal with one phenolate oxygen, one amine nitrogen and two bridging oxygen atoms [N(2),O(1),O(2), O(4) around Cu(1) and N(4), O(3), O(2), O(4) around Cu(2)] defining a square basal plane; the remaining amine N atoms N(1) (at Cu1) and N(2) [at Cu(2)] occupy the apical sites. The coordination pattern of **H_2L3** ligand in complex **3** is different from that of **H_2L2** in complex **2**

Table 6. Selected bond lengths [Å] and angles (°) for complex $[Zn_2(L2)_2]$ **(2)**.

Bond lengths [Å]			
Zn(1)-O(1)	1.95(4)	Zn(1)-N(2)	2.17(3)
Zn(1)-O(2)	1.99(3)	Zn(1)-N(1)	2.17(3)
Zn(1)-O(3)	2.04(3)	Zn(2)-N(4)	2.15(4)
Zn(2)-O(4)	1.93(3)	Zn(2)-N(3)	2.19(3)
Zn(2)-O(3)	1.99(3)	Zn(1)-Zn(2)	3.15(7)
Zn(2)-O(2)	2.04(3)		
Bond angles (°)			
O(1)-Zn(1)-O(2)	117.63(1)	O(1)-Zn(1)-O(3)	103.99(1)
O(2)-Zn(1)-O(3)	77.21(1)	O(1)-Zn(1)-N(2)	119.21(1)
O(2)-Zn(1)-N(2)	123.04(1)	O(3)-Zn(1)-N(2)	92.60(1)
O(1)-Zn(1)-N(1)	93.23(1)	O(2)-Zn(1)-N(1)	91.22(1)
O(3)-Zn(1)-N(1)	162.28(1)	N(2)-Zn(1)-N(1)	82.40(1)
O(4)-Zn(2)-O(3)	114.19(1)	O(4)-Zn(2)-O(2)	106.58(1)
O(3)-Zn(2)-O(2)	77.28(1)	O(4)-Zn(2)-N(4)	114.38(1)
O(3)-Zn(2)-N(4)	131.22(1)	O(2)-Zn(2)-N(4)	93.18(1)
O(4)-Zn(2)-N(3)	94.23(1)	O(3)-Zn(2)-N(3)	90.12(1)
O(2)-Zn(2)-N(3)	158.67(1)	N(4)-Zn(2)-N(3)	82.16(1)
C(1)-O(1)-Zn(1)	115.60(3)	C(15)-O(2)-Zn(1)	122.8(2)
Zn(1)-O(2)-Zn(2)	102.65(1)	Zn(2)-O(3)-Zn(1)	102.81(1)
C-H...π interactions (Å):			
C–H...$Cg'_{(4mp)}$	3.27(2)	C–H...$Cg'_{(4mp)}$	3.13(2)

Table 7. Selected bond lengths [Å] and angles (°) for complex $[Cu_2(L3)_2].CH_2Cl_2$ **(3)**.

Bond lengths [Å]			
Cu(1)-O(1)	1.87(1)	Cu(2)-N(4)	2.41(1)
Cu(1)-O(2)	1.96(1)	Cu(1)-N(1)	2.06(1)
Cu(1)-O(4)	2.00(1)	Cu(2)-N(3)	2.07(1)
Cu(2)-O(3)	1.88(1)	Cu(1)-N(2)	2.48(1)
Cu(2)-O(4)	1.94(1)	Cu(1)-Cu(2)	2.99(4)
Cu(2)-O(2)	2.02(1)	Cl(1)-C(49)	1.74(3)
		Cl(2)-C(49)	1.75(3)
Angles (°)			
Cu(1)-O(2)-Cu(2)	97.49(6)	Cu(2)-O(4)-Cu(1)	98.74(6)

Table 8. C–H…π interactions (Å).

C–H…$Cg'_{(2,4dmp)}$	3.19(1)	C–H…$Cg''_{(2,4dmp)}$	2.75(1)

although both complexes have similar square pyramidal geometry around the metal centre. The axial site is occupied by phenolate oxygen [O(1) and O(4)] in complex **2** while in complex **3**, the axial position is coordinated by amine nitrogen [N(2) and N(4)] in square pyramidal geometry. In complex **3**, the dihedral angle between two basal plane [N(2)O(1)O(2)O(4)Cu(1) and N(4)O(3)O(2)O(4)Cu(2)] is 51.02(16)°.

The Cu–O bond distances in complex **3**, which fall in the range 1.866(3)–2.016(3) Å, are in agreement with that of reported for similar copper(II) systems.[36–38] The Cu–N (equatorial) bond length range between 2.066(16) and 2.079(16) Å are comparable with the corresponding values obtained for similar Cu(II)-diamine complexes.[36–38] The Cu–N (axial) bond lengths range between 2.483(16) and 2.413(16) are also comparable to those reported for Cu(II)-diamine complex.[39] The shortening of the Cu–N (equatorial) bond length [2.066(16)–2.079(16) Å] in comparison to Cu–N(axial) distances [2.1413(16)–2.483(16) Å] is typical for a d^9 configuration of the Cu(II) ion.

The Cu…Cu distance within molecule is 2.999(4) Å, which falls within the range of known Cu…Cu distances in double-bridged copper polynuclear systems.[36–38] The bridged angle Cu(1)…O(1)…Cu(2) and Cu(1)…O(2)…Cu(2) are 97.49(16)° and 98.74(16)°, respectively. It should be noted that the structure of complex **3** is almost identical to that of a Cu(II) complex derived from ligand **H_2L1** reported in the literature.[39] The crystal structure of complex **3** reveals the existence of C–H…π due to the presence of co-crystallized molecule CH_2Cl_2. There are two types of C–H…π interactions, one occurring between a hydrogen (H49A) of methylene group (C49-H49A) and π electrons of 2,4-dimethylphenol ring (Cg' = C9C10C11C12C13C14) and second one between other hydrogen (H49B) of the same methylene (C49-H49B) group and π electron of another 2,4-dimethylphenol ring (Cg'' = C25C26C27C28C30). The distance between C–H…Cg' and C–H…Cg'' are 3.190 Å and 2.757 Å, respectively (figure 5b). The C–H…Cg'' interaction is stronger than the C–H…Cg'.

3.3 *Phosphotriesterase activity of complexes **1–3***

The PTE activity of complexes **1–3** was studied by employing ^{31}P NMR spectroscopic methods. Interestingly, complex **1** exhibited high PTE activity by hydrolysing the phosphotriester substrate PNPDPP (scheme 3) and a complete hydrolysis took place within 2 h, when 20 mM of the catalyst and 20 mM of PNPDPP were used (figure S18). The ^{31}P NMR spectra indicate that the peak at −18.32 ppm for the phosphotriester disappeared completely to produce a new signal at −10.73 ppm for diester. A further conversion of diester to monoester was not observed (figure S18). Complex 1 also showed methanolysis

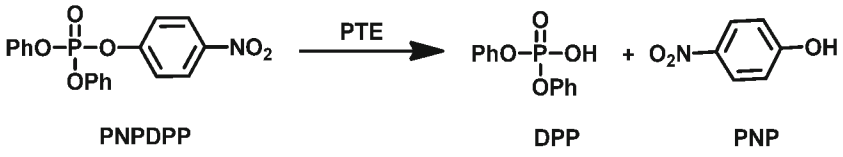

Scheme 3. Hydrolysis of phosphotriester (PNPDPP) to diphenylphosphate (DPP) and *p*-nitrophenol (PNP) in the presence of PTE.

of PNPDPP at ambient temperature, when methanol was used for the reaction (figure S17). The zinc complex **2**, which does not contain any water molecule in coordination around metal centre, was not able to hydrolyse PNPDPP in methanol (figure S19). Similarly, complex **2** was found to be inefficient in hydrolysing PNPDPP in CHES buffer at pH 9.0 (figure S20), although the metal ion can generate a nucleophilic metal-bound hydroxide in CHES buffer/aqueous medium. However, the Zn–OH species required for the hydrolysis appears to be absent in both methanol/CHES buffer medium. This is presumably due to the high stability of the complex **2** in aqueous/methanolic medium. In contrast to complex **1**, the binuclear complex **2** was found to be a poor mimic of PTE. In buffer, complex **2** was able to convert only a small amount of PNPDPP to diphenylphosphate after ~3 h (figure S20). Similarly, the binuclear Cu(II) complex **(3)** was also found to be a poor mimic of PTE as compared to complex **1** (figure S22). As complex **3** is capable of generating metal-bound hydroxide in buffer, the conversion of PNPDPP to DPP took place within ~2 h. However, the conversion of PNPDPP to DPP by complex **3** was found to be significantly slower than that of complex **1**. The binuclear Cu(II) complex was not able to hydrolyse PNPDPP in methanol (figure S21). The ^{31}P NMR studies indicate that the mononuclear Zn(II) complex **1** exhibits significant PTE activity due to the presence of coordinated water molecule at the Zn(II) centre. The possible mechanism for the PTE activity by mononuclear Zn(II) complex **(1)** was studied by mass spectrometry. Mass spectrometric analysis indicated that the complex **1** forms a catalyst-substrate complex [Zn(L1-OH)PNPDPP] (**1.1**) in order to hydrolyse PNPDPP in CHES buffer at pH 9.0. The Zn(II)-catalysed methanolysis of phosphotriester has been previously reported by Brown and coworkers.[40] Similarly, complex **1** may activate methanol to methoxide, which can attack the electrophilic phosphorus centre of PNPDPP and cleaves the phosphotriester bond leading to the generation of diphenyl ester.[19] The free ligand **H_2L1-H_2L3** and simple metal salts ($ZnCl_2$ and $CuCl_2$) did not show any noticeable activity in methanol as well as in buffer. The activity of complex **1** and **3** can be ascribed to the presence of an activated Zn–OH/Cu(II)–OH species in buffer. It should be mentioned that the stability of the complexes in buffer/water is crucial for the hydrolytic activity of synthetic compounds. Certain active zinc(II) complexes that exhibit aminopeptidase activity are deactivated in the presence of water[41]. Although the dinuclear Zn(II) complex **(2)** is quite stable in buffer condition, it is inefficient in hydrolysing the triester completely. However, although complex **2** is efficient in hydrolysing phosphotriester, we could not detect any peak for the diester due to the insolubility of the catalyst-substrate complex/diester in the CHES buffer. On the other hand, complex **3** shows different behaviour in methanol and buffer. While this complex is inactive in methanol (figure S21), it exhibited good PTE activity in CHES buffer. The mechanism is consistent with the report of Lippard *et al*[42] that the rate limiting nucleophilic attack of the hydroxo species at the substrate followed by fast protonation of the intermediates leads to the formation of the hydrolysed product.

3.3a *Interaction of phosphotriester with complex **1***: To further understand the binding of phosphotriester to the zinc(II) complex **1**, we have carried out the hydrolysis of PNPDPP by complex **1** in CHES buffer at pH 9.0 and the reactions were monitored by ^{31}P NMR spectroscopy and ESI-MS techniques. The mass spectrum of the reaction mixture indicated the formation of an intermediate complex [Zn(L1)-OHPNPDPP)] (**1.1**). The formation of complex **1.1** was further confirmed by MS-MS fragmentation of the parent ion. The ^{31}P NMR spectrum also indicted the formation of complex **1.1**. The chemical shift observed for this complex (−3.31 ppm) is shifted downfield as compared to that of diphenylphosphate, indicating that the triphenylphosphate binds strongly to the mononuclear metal ion centre. This observation clearly suggests that the M(II)-hydroxo species formation in buffer is responsible for the observed PTE activity. According to this mechanism, the coordinated water to Zn(II) metal ion centre is converted to a Zn–OH species at pH 9.0 in buffer solution. An attack of the nucleophilic –OH at the P=O centre leads to the formation of intermediate complex **1.1**. A peak at −11.56 ppm in ^{31}P NMR spectrum can be assigned to the catalyst-substrate complex (**1.1**). The nucleophilic attack of zinc(II) bound hydroxide at the phosphorous centre leads to the elimination of *p*-nitrophenol. In the case of binuclear Zn(II) complexes, the mass spectral analysis indicated that PNPDPP does not bind strongly to Zn(II) metal ion centre. Similarly, we were not able to obtain MS-MS fragmentation of Cu(II) complex, probably due to insolubility of the intermediate complex in CHES buffer.

4. Conclusions

In this paper, we have described the synthesis of some symmetrical *bis*-phenolate ligands containing the N_2O_2

donor sites and their corresponding mono/binuclear Zn(II) and Cu(II) complexes. The complexes presented in this report demonstrate the ability of the ONNO donor sites of ligands to Zn(II) and Cu(II) metal ions. These complexes were studied for the PTE activity. Among three complexes tested, the mononuclear Zn(II) having one water molecule at metal centre and a binuclear Cu(II) complex exhibit PTE activity. The binuclear Zn(II) complex is not efficient in hydrolysing PNPDPP to diester, which can be ascribed to the inability of this complex to generate a metal-bound hydroxide. In agreement with our previous studies on PTE mimics, mononuclear Zn(II) complexes having activated water molecules can exhibit significant PTE activity.

Supplementary material

The supplementary data include ^{1}H and ^{13}C NMR and mass spectra of the ligands **H_2L1**, **H_2L2**, **H_2L3** and complexes **1**–**3** (figures S1–S24).

Acknowledgements

This study was supported by the Department of Science and Technology (DST), New Delhi. GM acknowledges the DST for the award of Swarnajayanti Fellowship. MS thanks the University Grant Commission (UGC), New Delhi, for Dr. D S Kothari Postdoctoral Fellowship. JPJ acknowledges the (NSF-MRI) National Science Foundation- Major Research Instrumentation Program (grant no. CHE1039027) for funds to purchase the X-ray diffractometer.

References

1. Williams R J P 1989 in *Zinc in human biology* (ed): C F Mills, Berlin, Germany: Springer-Verlag p 15
2. Vallee B L 1986 in *A synopsis of zinc biology and pathology in zinc enzymes* (ed): Gray H B Boston: Bertini, Birkhauser 1
3. Vahrenkamp H 2007 *Dalton Trans.* **42** 4751
4. (a) Holm R H, Kennepohl P and Solomon E I 1996 *Chem. Rev.* **96** 2239; (b) Vallee B L and Neurath H 1954 *J. Am. Chem. Soc.* **76** 5006; (c) Vallee B L and Auld D S 1993 *Acc. Chem. Res.* **26** 543; (d) Vallee B L and Auld D S 1990 *Biochemistry* **29** 5647; (e) Sträter N, Lipscomb W N, Klabunde T and Krebs B 1996 *Angew. Chem. Int. Ed. Engl.* **35** 2025; (f) Steinhagen H and Helmchem G 1996 *Angew. Chem. Int. Ed. Engl.* **108** 2489; (g) Wilcox D E 1996 *Chem. Rev.* **96** 2435
5. Lipscomb W N 1970 *Acc. Chem. Res.* **3** 81
6. Nelson D E and Young K D 2001 *J. Bacteriol.* **183** 3055
7. Abraham E P and Chain E 1940 *Nature* **46**(3713) 837
8. Kim E E and Wyckoff H W 1991 *J. Mol. Biol.* **218** 449
9. Dong Y-J, Bartlam M, Zhou L S-F, Zhang Z-P, Zhang C-G, Rao Z and Zhang X-E 2005 *J. Mol. Biol.* **353** 655
10. Barr D B, Bravo R, Weerasekera G, Caltabiano L M, Whitehead R D, Olsson A O, Caudill S P, Schober S E, Pirkle J L, Sampson E J, Jackson R J and Needham L L 2004 *Environ. Health Perspect.* **112** 983
11. Casida J E and Quistad G B 2004 *Chem. Res. Toxicol.* **17** 983
12. Dragun J, Kuffner A C and Schneiter R W 1984 *Chem. Eng.* **91** 65
13. Benning H M, Shim H, Rausel F M and Holden H M 2001 *Biochemistry* **40** 2712
14. Lotti M 2002 *Toxicology* **181** 245
15. Singh B K 2009 *Nat. Rev. Microbiol.* **7** 756
16. (a) Sethunathan N and Yoshida T J 1973 *Microbiology* **19** 873; (b) Serdar C M, Gibson D T, Munnecke D M and Lancaster J H 1982 *Appl. Environ. Microbiol.* **44** 246; (c) Amitai G, Adani R, Sod-Moriah G, Rabinovitz I, Vincze A, Leader H, Chefetz B, Leibovitz-Persky L, Friesem D and Hadar Y 1998 *FEBS Lett.* **438** 195; (d) Shim H and Raushel F M 2000 *Biochemistry* **39** 7357
17. (a) Kazankov G M, Sergeeva V S, Efremenko E N, Alexandrova L, Varfolomeev S D and Ryabov A D 2000 *Angew. Chem. Int. Ed.* **39** 3117; (b) Kuo L Y and Perera N M 2000 *Inorg. Chem.* **39** 2103; (c) Barr L, Easton C J, Lee K, Lincoln S F and Simpson J S 2002 *Tetrahedron Lett.* **43** 7797; (d) Kim M, Liu Q and Gabbai F P 2004 *Organomettalics* **34** 5560; (e) Klinkel, K L, Kiemele L A, Gin D L and Hagadorn J R 2006 *Chem. Commun.* **27** 2919
18. Chanda A, Khetan S K, Banerjee D, Ghosh A and Collins T J 2006 *J. Am. Chem.Soc.* **128** 12058
19. (a) Tamilselvi A and Mugesh G 2006 *Chem. Eur. J.* **12** 7797; (b) Tamilselvi A and Mugesh G 2008 *J. Biol. Inorg. Chem.* **13** 1039; (c) Tamilselvi A and Mugesh G 2010 *Chem. Eur. J.* **16** 8878; (d) Umayal M and Mugesh G 2011 *Inorg. Chim. Acta* **372** 353
20. (a) Vaidyanathan M, Vaidyananthan M V and Palaniandavar M 2000 *Proc. Indian Acad. Sci. (Chem. Sci.)* **112** 223; (b) Maity D, Sheldrick W S, M-Figge H and Ali M 2007 *Indian J. Chem. Sect. A* **46** 1057; (c) Haasan K, Fowler C, Kwong P, Crane A K, Collins J L and Kozak C M 2008 *Dalton Trans.* **22** 2991; (d) Higham C S, Dowling D P, Shaw J L, Cetin A, Ziegler C J and Farrell J R 2006 *Tetrahedron Lett.* **47** 4419
21. (a) Nagataki T and Itoh S 2007 *Chem. Lett.* **36** 748; (b) Rodriguez L, Labisbal E, Sousa-Pedrares A, Garcia-Vazquez J A, Romero J, Duran M L, Real J A and Sousa A 2006 *Inorg. Chem.* **45** 7903
22. (a) Philibert A, Thomas F, Philouze C, Hamman S, Saint-Aman E and Pierre J-L 2003 *Chem.-Eur. J.* **9** 3803; (b) Rotthaus O, Thomas F, Jarjayes O, Philouze C, Saint-Aman E and Pierre J-JL 2006 *Chem.-Eur. J.* **12** 6953
23. John A, Shaikh M M and Ghosh P 2008 *Dalton Trans.* **22** 2815
24. Tshuva E Y, Goldberg I, Kol M and Goldschmidt Z 2001 *Organometallics* **20** 3017
25. Habbadi N, Dartiguenave M, Lamande L, Sanchez M, Simard M, Beauchampd A L and Souiria A 1998 *New. J. Chem.* **22** 983

26. Oxford Diffraction 2007 CrysAlis RED and CrysAlis CCD Versions 1.171.31.8, Abingdon, Oxafordshire, England: Oxford Diffraction Ltd
27. Sheldrick G M 1996 *Acta Crystallogr. Sect. A* **46** 467
28. Sheldrick G M 1997 *SHELXL-97, Program for crystal structure refinement*, Germany: University of Göttingen
29. Sheldrick G M 2001 *SADABS, Version 2, Multi scan absorption correction program*, Germany: University of Göttingen
30. Johnson C K 1976 *ORTEP*-II, Report ORNL-5138, Oak Ridge National Laboratory, Oak Ridge TN
31. (a) Sorrell T N, O'Connor C J, Anderson O P and Reibenspies J H 1985 *J. Am. Chem. Soc.* **107** 4199; (b) Nasir M S, Cohen B I and Karlin K D 1992 *J. Am. Chem. Soc.* **114** 2482
32. Howard R H, Bochmann M and Wright J A 2006 *Acta Crystallogr. Sect. C* **62** m293
33. Wang F-Q, Zheng X-J and Sun Y-X 2009 *Bull. Korean Chem Soc.* **30** 264
34. Nayak M, Sarkar S, Hazra S, Sparkes H A, Howard J A K and Mohanta S 2011 *Cryst. Eng. Commun.* **13** 124
35. Anjos A D, Bortoluzzi A J, Szpoganicz B, Caro M S B, Friedermann G R, Mangrich A S and Neves A 2005 *Inorg. Chim. Acta* **358** 3106
36. Saimiya H, Sunatsuki Y, Kojima M, Kashino S, Kambe T, Hirotsu M, Akashi H, Nakajima K and Tokii T 2002 *J. Chem. Soc. Dalton Trans.* 3737. http://pubs.rsc.org/en/Content/ArticleLanding/2002/DT/b201741e
37. Wang S, Pang Z and Smith K D L 1993 *Inorg. Chem.* **32** 4992
38. Lonnon D G, Colbran S B and Craig D C 2006 *Eur. J. Inorg. Chem.* 1190. http://onlinelibrary.wiley.com/doi/10.1002/ejic.200501063/pdf
39. Mijanuddin M D, Jana A D, Drew M G B, Hong C S, Chattopadhyay B, Mukherjee M, Nandi M, Bhaumik A, Helliwell M, Mostafa G and Ali M 2009 *Polyhedron* **28** 665
40. Desloges W, Neverov A A and Brown R S 2004 *Inorg. Chem.* **43** 6752
41. Sakiyama H, Mochizuki R, Sakamoto A, Nishida Y and Yamasaki M J 1999 *Chem. Soc. Dalton Trans.* **6** 997
42. Kaminskaia N V, He C and Lippard S J 2000 *Inorg. Chem.* **39** 3365